The Compact High Resolution Imaging Spectrometer (CHRIS): the future of hyperspectral satellite sensors. Imagery of Oostende coastal and inland waters

Barbara Van Mol[a] and Kevin Ruddick[a]

[a] Management Unit of the North Sea Mathematical Models (MUMM), Royal Belgian Institute for Natural Sciences (RBINS), Gulledelle 100, B-1200 Brussels,
email: B.Vanmol@mumm.ac.be, K.Ruddick@mumm.ac.be

ABSTRACT

The gap between airborne imaging spectroscopy and traditional multi spectral satellite sensors is decreasing thanks to a new generation of satellite sensors of which CHRIS mounted on the small and low-cost PROBA satellite is the prototype. Although image acquisition and analysis are still in a test phase, the high spatial and spectral resolution and pointability have proved their potential. Because of the high resolution small features, which were before only visible on airborne images, become detectable. In particular coastal waters very close to the shore and inland waters become visible, opening up potential new application areas. This article gives a description of the CHRIS/PROBA system and compares it with a ocean color satellite sensors and airborne imaging spectrometers. A CHRIS image of the coastal waters of Oostende is used here to map suspended particulate matter. Analysis of imagery for an inland water body suggests that the near infrared (NIR) wavelengths are strongly affected by adjacency effects (environmental straylight).

Keywords: CHRIS, PROBA, hyperspectral, satellite sensor, image spectroscopy, airborne, SPM, adjacency.

1 INTRODUCTION

Water, sand, plants, phytoplankton, etc. differ in the way they reflect light of different wavelengths. The human eye perceives these differences as color and the color of water, therefore, differs according to which and how much material is suspended or dissolved in the water. To get an accurate idea of the color of the water, spectral data - usually collected by satellite-borne ocean color sensors - are used. Traditional ocean color sensors collect light in a small number (varying from 8 bands for SeaWiFS to 15 bands for MERIS and 16 bands for MODIS) of relatively broad spectral bands. This is adequate for mapping phytoplankton (represented by chlorophyll-a concentration) in oceanic waters. However for coastal waters the optical complexity of both the sea and the atmosphere necessitates as much spectral information as possible to distinguish unambiguously between the various optically active substances. The first generation of hyperspectral imaging sensors was airborne. These optical remote sensing systems can provide image data with detailed spectral resolution, e.g. up to 288 (CASI 2 [1]) spectral bands, and are powerful tools for earth observation [2, 3]. However, airborne image spectrometry has some disadvantages compared with satellite based image spectroscopy of which the reduced swath is one.

A new generation of satellite sensors and platforms with a spectral and spatial resolution intermediate to airborne and traditional satellite imaging spectrometers is beginning to appear. These satellite based hyperspectral imaging spectrometers will reduce the gap between space- and airborne imaging spectroscopy. A prototype is the CHRIS/PROBA system, described here. CHRIS images are analyzed here for the Oostende test site to determine the feasibility of mapping Suspended Particulate Matter (SPM) and Chlorophyll a.

2 CHRIS/PROBA

CHRIS is an imaging spectrometer, carried on board of a space platform called PROBA (Project for On Board Autonomy). PROBA carries the instrument in a sun-synchronous elliptical polar orbit, at a mean altitude of about 600 km. The satellite was successfully launched [4] in October, 2001. CHRIS/PROBA distinguishes itself from other satellite imaging spectrometers by its physically compact payload, its high spatial and spectral resolution and pointability: when PROBA's across track pointing ability is used, all parts of the Earth's surface are accessible. For a chosen target, 5 images with different viewing angles (-55°, -36°, 0°, 36° and 55°) are made in a time period of 2.5 minutes (figure 2).

Presented at the Airborne Imaging Spectroscopy Workshop, Bruges, 8 October 2004

2.1 CHRIS: Compact high resolution imaging spectrometer

The name CHRIS summarizes the instrument:

- **C**ompact: it weighs less than 15 kg and has a volume of 790x260x200mm.
- **H**igh **R**esolution: it has a maximal spatial resolution of 18m if only 19 spectral bands are used and a minimum of 36 m for 63 spectral bands. CHRIS has 63 spectral bands with a minimum width of 1.3 nm at wavelength 410 nm and a maximum width of 12 nm at 1050 nm. A CHRIS image has a swath of about 14 km (this is somewhat variable as the altitude varies around the orbit).
- **I**maging **S**pectrometer: defined as a "class of instruments which preserve the image field while also determining the spectrum" [5]. The telescope in the CHRIS instrument is nadir pointing.

Figure 1. The CHRIS instrument (developed by Sira Electro-Optics Ltd.)

Because of a finite data transfer rate between the ground station and the platform the number of bands that can be output varies with the spatial resolution of the image [4]. The CHRIS band selection is programmable so that each application can use the most appropriate set of bands. In this test phase of CHRIS there are 5 principal configurations, based on a pre-launch wavelength calibration. For the Oostende test site mode 1 is used giving 62 spectral bands with a spatial resolution of 36m and a swath of 14km. More information about the CHRIS instrument can be found on www.chris-proba.org.uk.

2.2 PROBA: Project for On Board Autonomy

Proba is an advanced small satellite the size of a washing machine and weighing 94 kg. Its development has been led by the Belgian Verhaert consortium and supported by the European Space Agency (ESA). This satellite is pointable and has a high level of autonomy [6]. According to ESA: " Since its launch in 2001 Proba's high-performing computer system and technologically advanced instruments have enabled it to demonstrate and evaluate onboard operational autonomy, new spacecraft technology both hardware and software, and to test Earth observation and space environment instruments in space [7]." PROBA is a technology proving mission to test the potential and feasibility of such small satellites for advanced scientific and earth observation missions [4] and is considered as a forerunner for a new generation of small satellites. More specifications can be found on www.chris-proba.org.uk, www.esa.int and www.verhaert.com.

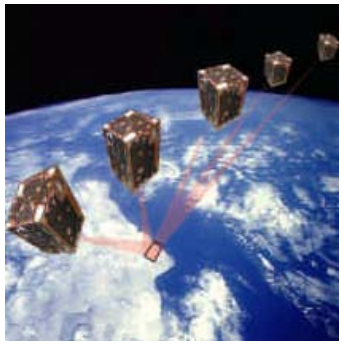

Figure 2. The pointability of the PROBA platform

3 COMPARISON OF OCEAN COLOR AND AIRBORNE SENSORS

Over the last few years the number of both satellite- and airborne hyperspectral sensors has increased enormously [8]. Some of the currently operational sensors are presented in table 1, but the list is not complete.

Table 1. Current sensor systems (in brackets: name of the satellite platform)[9, 10]

Ocean Color Sensors (more information on these sensors can be found on www.ioccg.org)	**Hyperspectral satellite sensors**	**Hyperspectral airborne sensors**
COCTS (HaiYang-1) MERIS (ENVISAT-1) MMRS (SAC-C) MODIS-Aqua (Aqua) MODIS-Terra (Terra) OCI (ROCSAT-1) OCM (IRS-P4) OSMI (KOMPSAT) SeaWiFS (OrbView-2)	FTHSI (MightySat II) Hyperion (EO-1) ARIES-I (ARIES-I) (expected launch 2005) CHRIS (PROBA) NEMO (COIS) (launch delayed)	AVIRIS HYDICE PROBE-1 Casi HyMap EPS-H DIAS 7915 DIAS 21115 AISA

While satellite platforms offer data at a global scale according to a systematic time schedule and with highly centralized data processing and distribution, airborne platforms offer the alternative of a more user-specific service at a regional scale. Data acquisition can be organized flexibly both in time and space [11].

In general currently operational ocean color satellite sensors have a large swath (> 800 km), a moderate spatial resolution (+/- 1 km) and a relative small number of bands (+/- 8 with an exception of 36 for MODIS). Airborne sensors typically have a high

spatial resolution (<1m – 10m), a large number of spectral bands (>200) and a small swath (<2km), with values depending on the height of the airplane and the sensor itself. The spectral coverage mostly varies from 400-480nm to 885-14385nm for both types. A comparison of the most important characteristics is made in table 2.

Table 2. Comparison traditional satellite based -, CHRIS and airborne imaging spectrometers [11, 1].

	Satellite based imaging spectrometers	CHRIS	Airborne imaging spectrometers
homogeneous data quality over a long time-frame	+	+	-
level of support	+	+/-	-
Entire earth is viewed with regular repetition	+	+/-	-
pointable	+	+	-
spatial resolution	-	+	+
geographical flexibility	-	+/-	+
spectral resolution	-	+	+
programmable spectral bands and pixel sizes	-	+/-	+

CHRIS/PROBA combines the advantages of satellite platforms (homogeneous quality long-term data suitable for highly automated processing) with a relatively high spatial and spectral resolution intermediate between ocean color satellite sensors and hyperspectral airborne sensors. CHRIS/PROBA could be "the future of hyperspectral satellite sensors" because of original technological features which may form the basis of a new generation of ocean color sensors:

- Economic constraints are likely to lead over the next twenty years to preference for small satellites with a very limited number of sensors (e.g. one) facilitating system design and launch. In this sense PROBA is seen as a model for a new generation of small low-cost satellites with consequent challenges for system engineers and for product developers.
- The optical complexity of coastal and inland waters and their overlying atmosphere drives a need for much greater spectral resolution than is available on current ocean color sensors, e.g. to separate phytoplankton absorption from colored dissolved organic matter (CDOM) absorption or to perform accurate atmospheric correction for turbid waters. It is becoming clear that the future for coastal and inland waters is hyperspectral and CHRIS thus offers a first chance to test future algorithms.
- Pointability of the platform allows imaging of the same sea area from different angles, thus offering

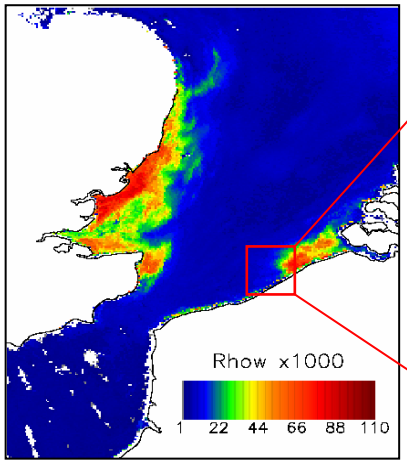

Figure 3. Unprocessed SeaWiFS image (5 August 2003) (670nm)

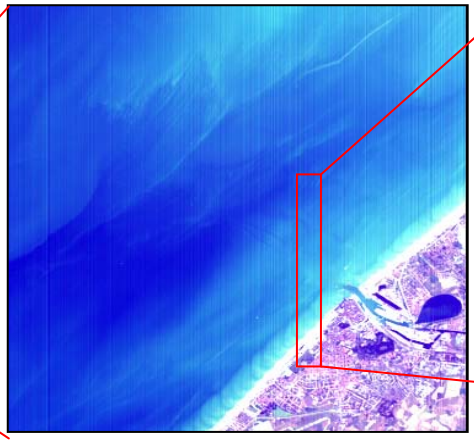

Figure 4. Unprocessed CHRIS image (21 September 2003) (R=691nm, G=561nm, B=442nm)

Figure 5. Unprocessed CASI image Oostende (16 June 2003) (R=643nm, G=551nm, B=461nm)

more information for use in correction of atmospheric and air-sea interface effects, as used by AATSR for sea surface temperature measurements. In a more general context pointable platforms offer the possibility of on-demand imaging for example in the case of special events, as used already for terrestrial applications in SPOT series.

- Finally, the high spatial resolution of CHRIS is more comparable to that of terrestrial sensors such as Landsat and SPOT than to that of ocean colour sensors (e.g.1.1 km for SeaWiFS, 250m for MERIS) and offers the possibility of mapping much smaller features for example in nearshore, estuarine or inland waters [12].

Figure 3, 4 and 5 shows respectively a SeaWiFS, CHRIS and CASI image with a swath with of 2800, 14 and 1.2 km and pixel sizes of 1100, 36, and 4m².

4 CHRIS IMAGES OF TESTSITE OOSTENDE

CHRIS images from the test site Oostende have been analyzed here to assess the feasibility of producing suspended particulate matter (SPM) and chlorophyll (CHL) maps.

The mode 1 configuration is used with a spatial resolution of 36*36m² and 62 spectral bands which cover wavelengths from 411 nm up to 997 nm.

As the image acquisition and analysis are still in a test phase, some problems need to be solved before converting the images into SPM and Chlorophyll maps including:

- vertical striping
- atmospheric correction
- georeferencing

To evaluate the correctness of the CHRIS data, the CHRIS-derived reflectance is compared with in situ measurements, MERIS and SeaWiFS data.

4.1. Destriping

Figure 6a shows the "vertical lines" on the image. These are especially visible at the lower wavelengths. By calculating and applying a correction factor based on a 5 column moving average, these "vertical lines" can be reduced. Figure 6b shows the same image as figure 6a but after destriping.

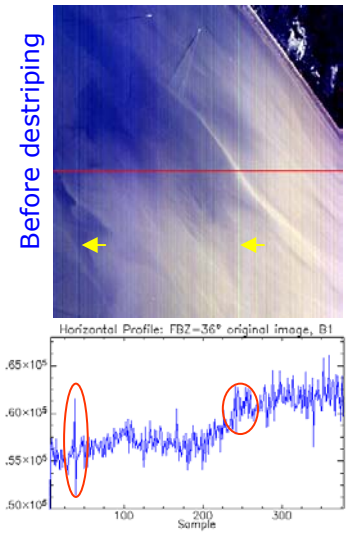

Figure 6a. Unprocessed CHRIS/PROBA image. 5 August 2003, FBZ = 36°, 411nm, top of atmosphere

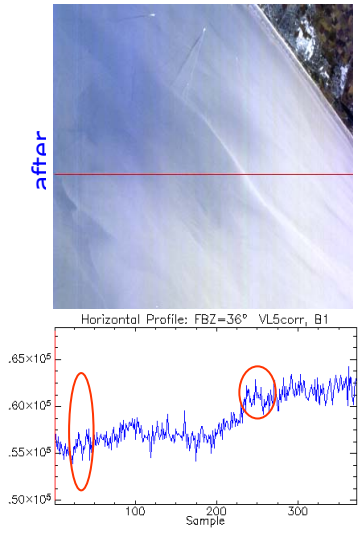

Figure 6b. Destriped CHRIS/PROBA image. 5 August 2003, FBZ = 36°, 411nm, top of atmosphere

4.2. Atmospheric correction

Although a radiative transfer model is a more accurate method to calculate the atmospheric correction, a darkest pixel approach is preferred because initially the images contain too much spectral noise to calculate all factors properly. This is a very simple correction, based on 2 assumptions:

- The first assumption is that in the darkest water pixel of the image there is total light absorption i.e. this pixel represents black water and the light recorded for this pixel is equal to the atmospheric path radiance.
- Secondly it is assumed that the atmospheric path radiance is uniform over the entire image.

The spectrum of the darkest water pixel (assumed to represent the atmosphere) is subtracted from the whole image. This results in spectra with a typical shape for water masses but because the water even in the darkest pixel is not perfectly black, there is an overestimation of the atmospheric path reflectance and an underestimation of the water leaving reflectance. The assumption of an equal atmosphere over the entire image site has less consequence on a clear day then on a partially clouded day. Despite such drawbacks the darkest pixel approach provides acceptable data.

4.3. Georeferencing

Georeferencing the CHRIS/PROBA satellite images is a major problem for marine sites because no georeferencing information is supplied with imagery and ground control points (GCP) cannot be identified at sea. The test site was chosen to contain some land for GCP identification.

Georeferencing images by the use of at least 4 ground control point (GCPs) on land gives a good result for the interpolated points on land but the error increases for extrapolated points far from the GCPs. This approach is not very accurate because all GCPs are located in the same corner of the image. The GCP location error for any image is typically half a pixel, if ground control points like for example a cross road, the corner of a bridge, a pool in a park are identified correctly. Here this uncertainty is amplified considerably going from the land corner of the image to the opposite sea corner.

The results of georeferencing the images are acceptable for the land and points close to land but information about georeferencing or even the nominal size, location and orientation of the image would lead to better results.

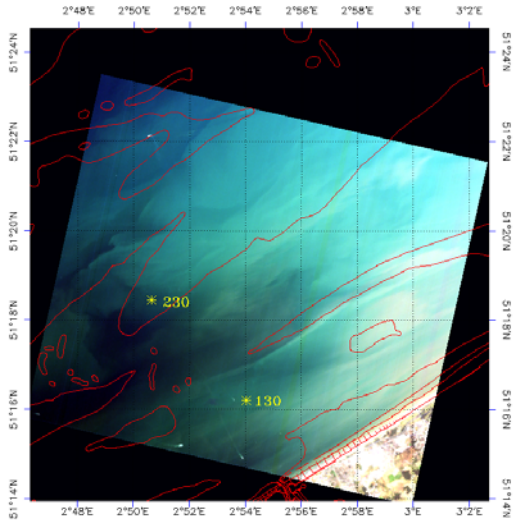

Figure 7. CHRIS image of 5 August 2003, FBZ = -36°, RGB composite using 691nm, 561nm and 461nm after image processing.

4.4. 5 August 2004

Since the launch of CHRIS/PROBA, 13 datasets of the core site Oostende have been acquired (table 3). Only the datasets acquired on 5 August 2003 and on 6 July 2004 were cloud free and have simultaneous seaborne measurements. The parameters measured are water-leaving reflectance, SPM and CHL.

Data of 5 August 2003 are compared with in-situ measurements taken at station 130 and 230 in Oostende waters (figure 7), while on the CHRIS data of 6 July 2004 the Spuikom (inland water) is studied.

4.4.1 Comparison with in situ data

Available match-up radiance and reflectance data are represented in table 4.

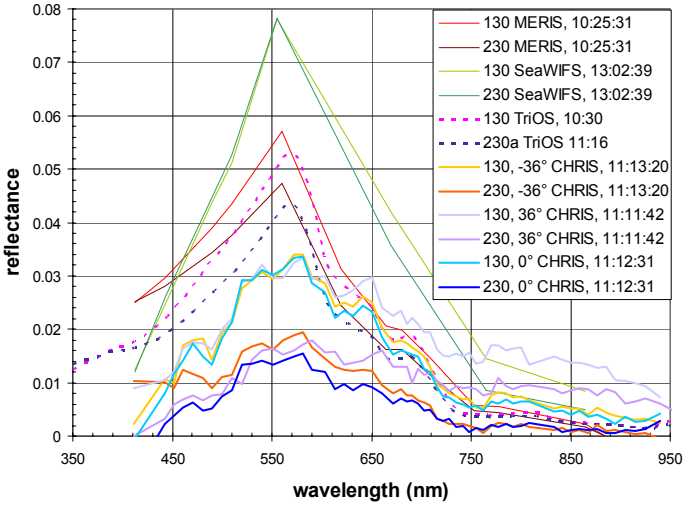

Figure 8. water-leaving radiance reflectance from seaborne and satellite measurements of 5 August 2003

Table 3. Data acquisition at the Oostende core site

Date	n° images	CHRIS data	Sea data
21/06/2002	5	clouded	4 stations
26/07/2002	5	clouded	2 stations
05/03/2003	5	clouded	No
19/06/2003	5	clouded	3 stations
27/06/2003	4	clouded	3 stations
21/07/2003	3	partially clouded	No
05/08/2003	5	clear	2 stations
06/08/2003	5	partially clouded	3 stations
20/09/2003	5	clear	No
21/09/2003	3	clear	No
14/06/2004	5	clouded	2 stations
21/06/2004	5	clouded	2 stations
06/07/2004	5	clear	2 station (Spuikom)

Table 4. Radiometric data acquired on 5 August 2003

Sensor	UTC time	latitude	longitude	FBZ
TriOS/station 130	10:30	51.27	2.90	
TriOS/station 230	11:16	51.31	2.84	
CHRIS/image A	11:11:42	51.28	2.88	36°
CHRIS/image 9	11:12:31	51.28	2.88	0°
CHRIS/image B	11:13:20	51.28	2.88	-36°
MERIS	10:25:31			
SEAWIFS	13:02:39			

Figure 8 presents the water leaving radiance reflectance spectra (defined as π times the above water

upwelling radiance corrected for air-sea interface reflection and divided by above water downwelling irradiance) at station 130 and 230 for the CHRIS/PROBA images with fly by zenith angles (FBZ) -36°, 0° and 36° (where positive is towards the sunglint direction) , TriOS, MERIS and SeaWIFS.

All sensors show a higher reflectance at station 130. This is explained by the concentration of particles in suspension at station 130 which leads to a higher reflection. Analysis of the water samples for SPM shows the same tendency (table 5).

The values are lower for CHRIS/PROBA in comparison with other sensor data. This can be explained by the darkest water pixel assumption. Time differences may also affect the comparison.

The CHRIS/PROBA spectra are similar at station 130 for wavelengths until 600nm for the 3 look angles. Higher wavelengths show a discrepancy for the data from the CHRIS/PROBA image with FBZ equal to -36°, possibly due to sunglint. The CHRIS/PROBA spectra at station 230 show more variation between the different view angles. These variations could be due to the increased georeferencing error further from land.

The CHRIS/PROBA radiance and reflectance spectra show spectral noise. This noise could be reduced by applying a spectral smoothing but because less is known about which values are correct and which are not, it is preferred at present not to smooth the spectra until good correction factors are available because important data could be lost.

4.4.2 SPM and CHL maps

- **SPM maps**

Figure 9 shows a SPM map deduced from the reflectance at wavelength 555 nm for CHRIS/PROBA images with fly by zenith angle -36°. SPM varies from +/- 4 to 25 mg/l. Remotely sensed SPM values using equation (11) of [12] with coefficient A_Q = 25.99 mg/l, B = 4.98 mg/l and C_Q = 0.187 are in the same range as the measured values (table 5).

Table 5. Satellite vs. seaborne measured SPM concentrations

Station	SPM (mg/l) FBZ = -36°	SPM (mg/l) FBZ = 0°	Measured SPM (mg/l)
130	11.41	11.35	8.20
230	7.98	7.16	7.27

Comparison with the SPM maps deduced from MERIS (figure 10) and SeaWiFS (figure 11) shows agreement and indicate that the strong SPM gradient across the CHRIS image corresponds to a frontal region between high SPM waters near the coast between Oostende and the Scheldt and low SPM waters offshore and further West. The stability of this feature over the 2.5 hour period considered and its appearance in many other SeaWiFS and MERIS images confirms that CHRIS detects successfully SPM.

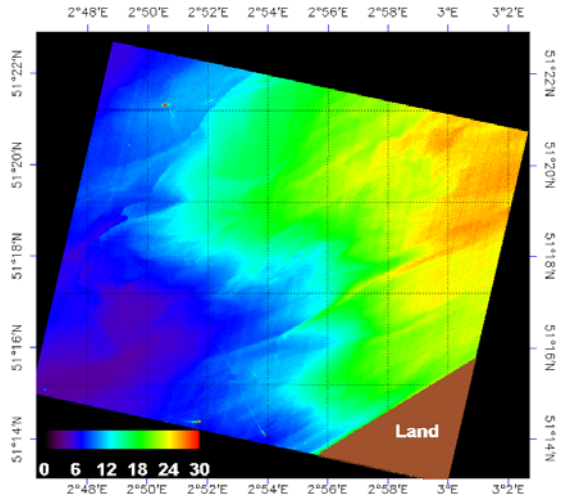

Figure 9. SPM map based on CHRIS/PROBA, 5 August 2003, FBZ = -36°, wavelength 551 nm

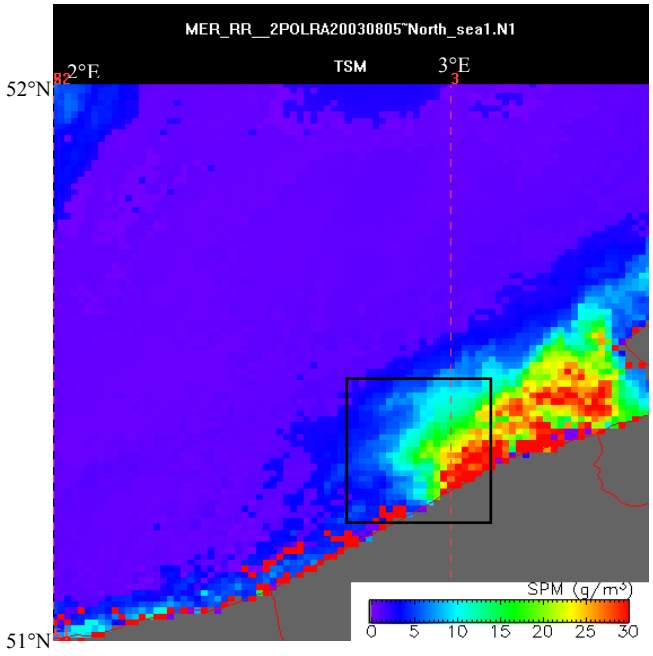

Figure 10. SPM map deduced from MERIS, 5 August 2003

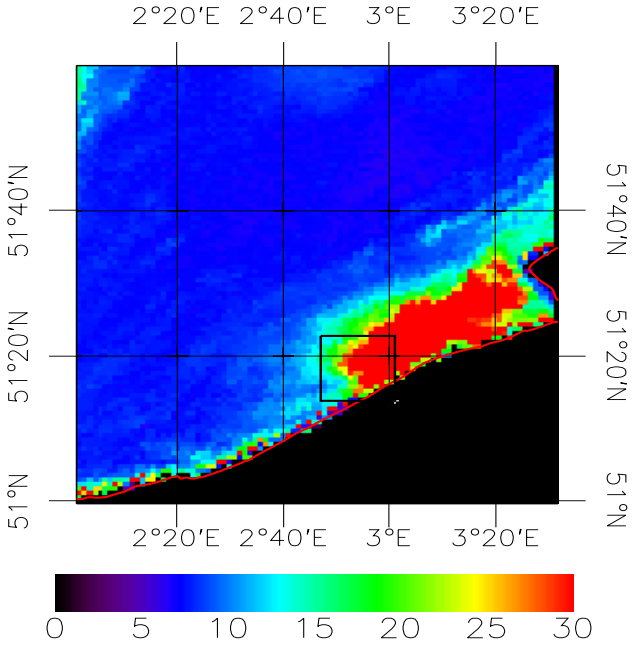

Figure 11. SPM map deduced from SeaWiFS, 5 August 2003

- **Chlorophyll maps**

The chlorophyll map in figure 12 is deduced from the CHRIS/PROBA image with FBZ -36° and is based on 3 bands: 664 nm, 708 nm and 778 nm as described in [13] and based on [14]. At first sight it seems it might be possible to create chlorophyll maps from CHRIS/PROBA images since the CHL distribution in figure 12 is not correlated with SPM nor with any obvious atmospheric feature. However, comparison with seaborne measurements and inspection of the highest values shows that the values are not realistic…yet (table 6).

Table 6. Satellite vs. water sample CHL concentrations

Station	Satellite value (mg/m³)	Measured value (mg/m³)
130	39.27	11.37
230	32.25	11.49

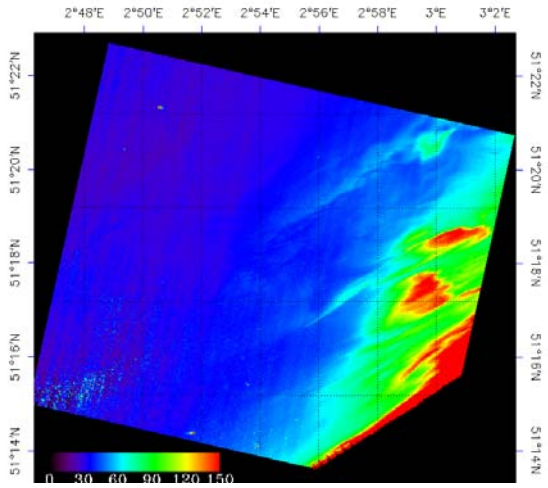

Figure 12. Chlorophyll map based on CHRIS/PROBA, 5 August 2003, FBZ = -36°

4.5 6 July 2004

On the CHRIS images of 6 July 2004, the Spuikom (an inland waterbody near the coast of Oostende) is studied.

In a previous study [13] and on figure 13 spectrum 5 the CHRIS water-leaving reflectance spectra at sea were found to have a shape comparable to seaborne measurements of water-leaving reflectance i.e. with reflectance decreasing almost monotonically from a peak in the range 550-600nm to values a factor 2 or more lower at 700nm with further decrease by a factor 2 or more to 800nm and a further decrease to 900nm because of the corresponding increase in pure water absorption. This spectral form, e.g. spectrum 5 of figure 13, is expected to be valid for all water bodies except perhaps for very shallow water (<1m) where the reflectance from the bottom may contribute to the surface reflectance at red and near infrared (NIR) wavelengths. Measurements of water-leaving reflectance from a small boat made in the turbid area of the Spuikom on 6th July 2004 confirm such a spectral shape. However, the atmospherically-corrected CHRIS data (spectra 1-4 in figure 13) depart very significantly from such a spectral form

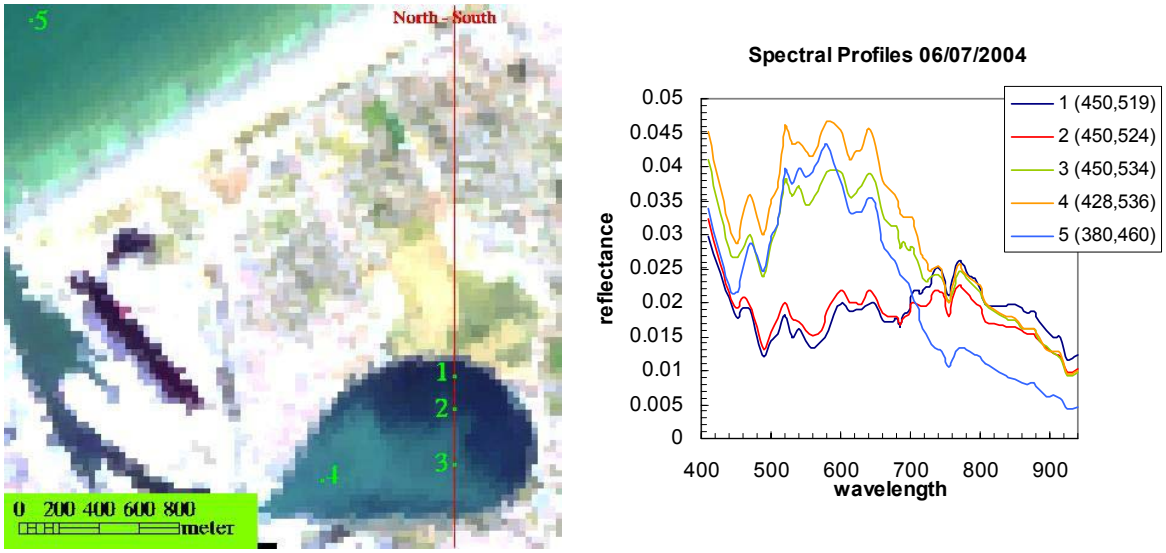

Figure 13. Reflectance spectra from CHRIS image of 6 July 2004, FBZ=0°, RGB composite using 691nm, 561nm and 461nm after image processing. Close-up of the Spuikom inland water body at Oostende.

for red and near infrared wavelengths. As depicted in figure 14, which shows the surface reflectance derived from CHRIS for the North-South line (figure 13) across the Spuikom, the reflectance at 777nm is in fact higher than at 651nm and 709nm in the North of the lake instead of being much lower as would be expected. Two hypotheses could explain such a high near infrared reflectance: bottom reflection or adjacency effects.

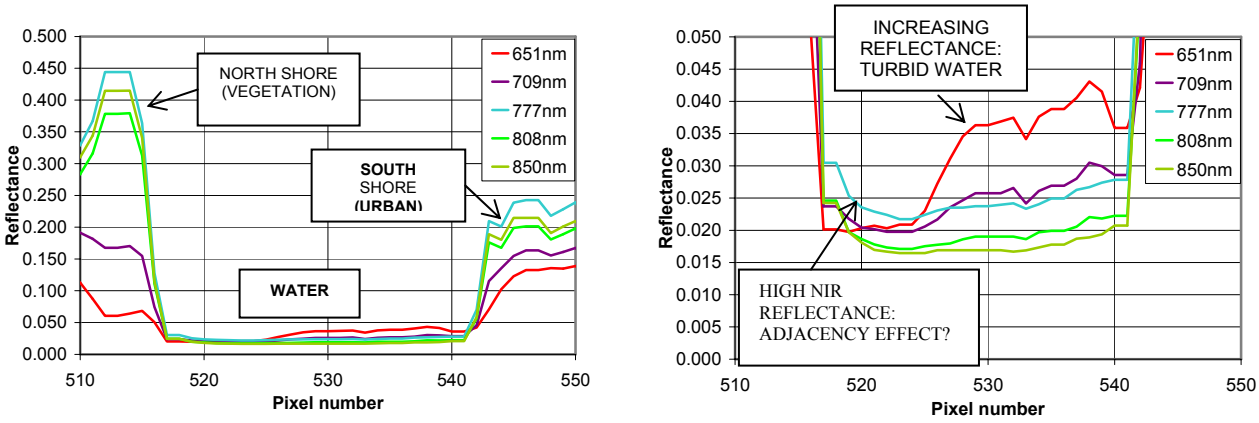

Figure 14. Profile of CHRIS surface reflectance across the Spuikom on 6th July 2004 from North (pixel 510) to South (pixel 550) along the line indicated in Figure 13

Visual and airborne observations confirm that the lake bottom is visible to the human eye for the less turbid Northern and Eastern parts of the lake. While such features will clearly affect the water-leaving reflectance for blue and green wavelengths, since they are visible to the human eye, bottom reflectance becomes rapidly absorbed for all but the shallowest water for red and near infrared wavelengths. For example the absorption of water is about $0.8m^{-1}$ at 709nm and rises to 4.2 m^{-1} at 850nm [15] with the result that even for clear water the surface signal of bottom reflectance is attenuated to a factor 0.45 and 0.015 or smaller at 709nm and 850nm respectively for water of 1m depth. Moreover these factors will be squared if the water depth doubles i.e. The bottom reflectance at 850nm is reduced to less than 0.022% of its bottom value by passage through water of 2m depth. Inspection of the decrease in reflectance for the wavelengths 709nm–850nm in the Northern portion of the Spuikom (i.e. from pixel number 518 to 524) shows a relatively similar decrease in reflectance for all wavelengths as water depth increases, which is contrary to the stronger decrease that would be expected at higher wavelengths for the case of bottom reflectance. This suggests that bottom reflectance cannot explain entirely the abnormally high reflectances found for these wavelengths.

According to the alternative hypothesis of adjacency effects (also called environmental straylight), some of the light reaching the sensor along the viewing direction for a water pixel could arise not from the water pixel itself but

from an adjacent land pixel after small angle forward scattering in the atmosphere. An alternative and similar effect could arise in the absence of atmospheric scattering from imperfect blocking by the sensor of light outside the instantaneous field of view [16], though it is thought that the CHRIS sensor is sufficiently focused to avoid such effects and that this is less likely than environmental straylight. The rapid and similar decrease of near infrared reflectances going away from the Northern shore of the lake is consistent with a decrease in atmospheric forward scattering (for increasing scattering angle) and the higher reflectances found for the water at 777nm as compared to 709nm, 808nm and 850nm are also consistent with a similar difference for the nearby vegetation on land. At the Southern shore adjacency effects are also likely to contribute to the surface reflectance signal though the more turbid water there tends to hide this signal (e.g. spectrum 3 in figure 13). The increase in reflectance at all wavelengths going from pixel 524 to 530 and the gradient of this increase (greater for lower wavelengths where water absorption is lower) is consistent with an increase in backscatter from particles in the water, as confirmed by visual observations.

5 CONCLUSION

The new generation hyperspectral imaging spectrometers carried on small satellite platforms of which CHRIS/PROBA is a prototype has significant potential for mapping SPM and chlorophyll and related parameters especially for nearshore and inland waters. The processing of CHRIS images involves some problems due to the data quality. Most of these problems are mitigated in the processing adopted here. The main problem in the processing of marine images is the georeferencing. CHRIS/PROBA image data are good enough to create useful SPM maps of the sea but the possibility to create CHL maps and to create reliable maps of inland waters needs further research.

The advantages of the different viewing angles are at this stage used only to eliminate sun glint. In the future the image set with different viewing angles may help to improve atmospheric correction or may be used as test data to validate sun glint algorithms e.g. for MERIS. The potential of multi-look angle hyperspectral imagery for suspended particulate matter and chlorophyll mapping remains promising but requires further assessment after improvement of image data and atmospheric correction.

The data derived from the CHRIS sensor for the inland water body is currently significantly contaminated in the near infrared, especially for clear water pixels. This contamination is consistent with small angle forward scattering of photons reflected from nearby land surfaces (adjacency effect), though a possible component from bottom reflectance cannot be completely ruled out in the shallowest waters. Further investigation of this process necessitates an improved atmospheric correction using a radiative transfer model and, if possible, a more precise spectral calibration of CHRIS. A more complete set of ground-level measurements is also needed, including sunphotometer measurement of atmospheric optical properties. Such measurements are planned in conjunction with an airborne campaign in the framework of the BRADEX experiment (Bottom Reflectance and Adjacency Experiment) and will provide a basis for correction of adjacency effects, which currently contaminate products from all ocean colour sensors for inland and nearshore waters, e.g. [17] for the case of MERIS. In this respect the high spatial and spectral resolutions of CHRIS provide significantly more information than is available from much more expensive operational systems such as Envisat-MERIS. CHRIS thus offers better opportunities for the development and validation of algorithms, to be applied in present and future operational systems for the correction of adjacency effects.

ACKNOWLEDGMENTS

This study was funded by the Belgian Science Policy Office in the framework of the BELCOLOUR project and by PRODEX contract 15189/01/NL/SFe(IC) The CHRIS/PROBA data was supplied by ESA/SIRA. The ESA/SIRA scientists and Peter Fletcher are thanked for their support. We thank Vera De Cauwer for the seaborne measurements of 5 August 2003 and the Tuimelaar crew for their help. MUMM's Chemistry lab is thanked for the chlorophyll/SPM analysis. Thanks go also to ESA, NASA and Orbimage for the MERIS and SeaWiFS data and to Youngje Park and Bouchra Nechad for processing them. Images of the CHRIS instrument, PROBA and the CASI images are respectively provided by Sira Technology Ltd, Frédéric Teston (PROBA Project Manager, ESTEC-D/TEC-EL) and Sindy Sterckx (VITO).

REFERENCES

[1] Innovation Technology Research Excellence Service: www.itres.com
[2] US Geological Survey Website: About Imaging Spectroscopy. http://speclab.cr.usgs.gov/aboutimsp.html

[3] Dekker, A.G., Brando, V.E., Anstee, J.M., Pinnel, N., Kutser, T., Hoogenboom, E.J., Peters, S., Pasterkamp, R., Vos, R., Olbert, C., Malthus, T.J.M., 2001. Imaging spectrometery of water. In: *Imaging Spectrometry*, van der Meer, F.D. and de Jong, S.M. (eds), Kluwer.
[4] CHRIS mission website: www.chris-proba.org.uk
[5] School of Information Technology and Engineering. http://www.site.uottawa.ca:4321/astronomy/index.html#imagingspectrometer
[6] Verhaert: http://www.verhaert.com
[7] PROBA, Project of Onboard Autonomy webpage (ESA) : http://www.esa.int/export/esaMI/Proba_web_site/ESAG9KTHN6D_0.html
[8] NIEKE, N., Schwarzer, H., Neumann, A., Zimmermann, G.: Imaging Spaceborne and Airborne Sensor Systems in the Beginning of the Next Century. In: SPIE, Vol: 3221.
[9] International Ocean-Colour Coordinating Group: www.ioccg.org
[10] Shippert, P., 2002: Spotlight on Hyperspectral. *Geospatial Solutions, February 1, 2002.* www.geospatial-online.com
[11] Ruddick, K., Lacroix, G., Park, J., Rousseau, V., De Cauwer, V., Debruyn, W., Sterckx, S., 2003: Overview of Ocean Colour : theoretical background, sensors and applicability for the detection and monitoring of harmful algae blooms (capabilities and limitations). *Submitted for the UNESCO Monographs on Oceanographic Methodology series, Manual on Harmful Marine Microalgae.*
[12] Nechad, B., De Cauwer, V., Park, Y., Ruddick, K., 2003: Suspended Particulate Matter (SPM) mapping from MERIS imagery. Calibration of a regional algorithm for the Belgian coastal waters. *European Space Agency. SP-549*
[13] Van Mol, B., Park, J., Ruddick, K., Nechad, B., 2004: Mapping of Chlorophyll and Suspended Particulate Matter Maps from CHRIS imagery of the Oostende core site. *2nd ESA/CHRIS Proba workshop. European Space Agency's Publication Division (EPD): Special Publication SP-578.*
[14] Gons, H.J., 1999. Optical teledetection of chlorophyll a in turbid inland waters. *Environmental Science and Technology. Vol. 33, p.1127-1133*
[15] Kou, L., Labrie, D. and Chylek, P., 1993. Refractive indices of water and ice in the 0.65µm to 2.5µm spectral range. *Applied Optics*, 32: 3531-3540.
[16] Robinson, I.S., 1985. Satellite Oceanography. Ellis Horwood Series in Marine Science. Ellis Horwood, Chichester, 455 pp.
[17] European Space Agency (ESA), 2003. MERIS Workshop User observations and recommendations. http://envisat.esa.int/workshops/meris03/MERIS_Workshop_reco4-2.pdf